# Microstructure of vinylidene fluoride and tetrafluoroethylene copolymers by high-resolution $^{19}F$ nuclear magnetic resonance

**G. Lutringer, B. Meurer* and G. Weill**
*Institut C. Sadron, CRM-EAHP, CNRS-ULP, 6 rue Boussingault, 67083 Strasbourg Cedex, France*
*(Received 13 November 1991; accepted 18 February 1992)*

Sequence analysis of soluble copolymers of various compositions of vinylidene fluoride and tetrafluoroethylene is performed based on $^{19}F$ nuclear magnetic resonance spectral intensities at very high field. A new strategy is proposed for the adjustment of a first-order Markov polymerization scheme to the experimental data. Previous line assignments are then discussed and minor lines arising from impurities can be eliminated.

**(Keywords: $^{19}F$ nuclear magnetic resonance; polymer microstructure; vinylidene fluoride; tetrafluoroethylene; copolymers; Markovian polymerization)**

## INTRODUCTION

Copolymers based on vinylidene fluoride ($VF_2$) have received increasing attention because of the role of the comonomer in inducing the ferroelectric $\beta$ phase and the existence of a ferro- to paraelectric transition below the melting point. A high fraction of head-to-head defects ($\simeq 11\%$) favouring the *trans* conformation[1] has been shown to be sufficient to induce crystallization of $PVF_2$ in the $\beta$ phase[2]. Similarly, copolymers of $VF_2$ with 7% tetrafluoroethylene ($VF_4$) crystallize in the $\beta$ phase[3]. A systematic study of the crystalline structure, melting point and Curie point of $VF_2$–$VF_4$ copolymers has been carried out at Bell Laboratories[4]. Copolymers with a $VF_4$ molar content between 7% and 17% crystallize in the $\beta$ phase but have decreasing melting temperatures, precluding the observation of a ferro- to paraelectric transition in the solid state. For $VF_4$ molar contents between 18% and 28% the melting temperature rises and a Curie point is observed. For $VF_4$ molar contents between 29% and 65% the ferro- and paraelectric phases seem to coexist in a large range of temperatures. The understanding of such properties requires a detailed description of the microstructure of the copolymers.

The $^{19}F$ n.m.r. spectrum of $VF_2$–$VF_4$ copolymers was first published by Wilson and Santee[5]. Murasheva[6] proposed an attribution of the 15 lines that appeared resolved at 84 MHz. A much higher resolution has since been obtained by Cais[7] at 470 MHz. The attribution of the 26 possible pentads was carried out not only on the basis of the chemical shifts but also from a comparison of the experimental and calculated intensities for a 12% and a 37% $VF_4$ molar content, using a first-order Markov copolymerization process based on the intensities of a few easy-to-assign lines.

We address essentially the same problem using a set of samples in a larger range of composition, a slightly modified scheme in the evaluation of the conditional probabilities of addition from the observed intensities, and an extended attribution of the lines. We thus discuss the evolution of the lengths of the $VF_2$ and $VF_4$ sequences in relation to the crystalline properties of these copolymers.

## MATERIALS AND METHODS

The $VF_2$–$VF_4$ copolymers have been prepared at Atochem Research Center by Pierre Bénite, with the exception of the very low $VF_4$ content copolymer (3.3%), which is a commercial Kynar product from Pennwalt. Their emulsion polymerization has been carried out under control of the monomer feed so that the final composition matches the initial monomer ratio and the polymer can be considered as homogeneous. Their theoretical compositions, as well as that determined by $^{19}F$ n.m.r. (see below), are given in *Table 1*. It also gives a molecular weight deduced from g.p.c. analysis in *N*-methylpyrrolidone (NMP) using a conversion from polystyrene (PS) calibration as found for $VF_2$ homopolymers[8].

$^1H$ (400 MHz) and $^{19}F$ (376 MHz) n.m.r. spectra have been recorded on a Bruker AM 400 spectrometer. Most experiments have been carried out on 6–8% (in weight) solutions in a 50/50 volume mixture of dimethylacetamide (DMAc) and perdeuterated dimethylformamide (DMF-$d_7$). A few experiments have been carried out in deuterated dioxane. This latter solvent shows increased resolution in $^1H$ resonance but lower resolution and line inversions in $^{19}F$ resonances. $^{19}F$ signals have been recorded under broad-band $^1H$ decoupling with a 16.6 kHz spectral width allowing use of a 16 bits digitizer.

* To whom correspondence should be addressed

0032-3861/92/234920-09

**Table 1** $VF_2$–$VF_4$ copolymer molar composition and mole weights

| Name | Mole weights, $VF_4$ content (%) Theor. | Meas. | $M_w$ | Reversed units (%) (from $^1H$ n.m.r.) |
|---|---|---|---|---|
| A | – | 3.3 | $290 \times 10^3$ | 5.4 |
| B | 9.3 | 9.2 | $154 \times 10^3$ | 3.9 |
| C | 18.5 | 19.8 | – | 3.6 |
| D | 19.6 | 21.4 | $155 \times 10^3$ | 3.5 |
| E | 21 | 21.3 | – | 3.5 |
| F | 22 | 22.4 | $104 \times 10^3$ | 3.5 |
| G | 28 | 28.0 | $85 \times 10^3$ | 3.0 |
| H | 30 | 31.6 | $239 \times 10^3$ | 3.0 |
| I | 37 | 37.7 | $183 \times 10^3$ | 2.2 |
| J | 47.5 | 47.8 | – | 2.0 |

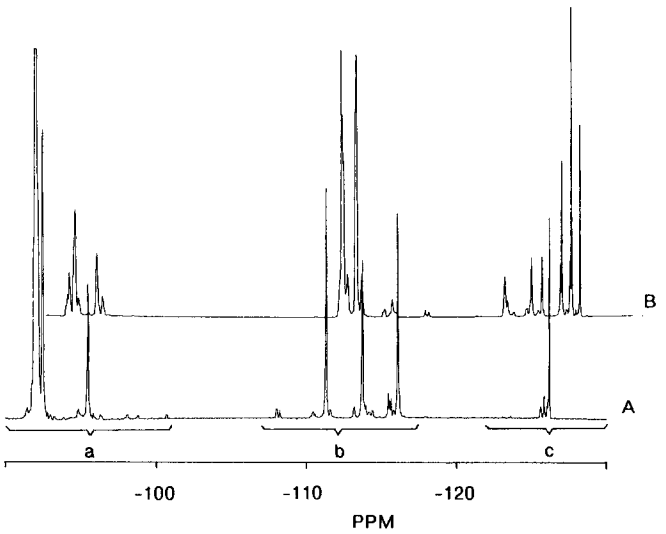


**Figure 1** $^{19}F$ n.m.r. spectra of copolymers 97/3 (A) and 63/37 (B)

Relaxation measurements indicate $T_1 < 0.7$ s for all lines; therefore a 3.5 $\mu$s 45° pulse and a delay time of 4–5 $T_1$ have been used to improve the signal-to-noise ratio. A typical recording time is 2 h. Chemical shifts are referenced from $CFCl_3$. Intensities are derived from the integrated values of the isolated lines or by decomposition of overlapping lines using the Bruker program LINESIM.

The Markov analysis of the polymerization kinetics from selected signal intensities and the recalculation of all line intensities have been carried out on the IBM 3090 of the CNRS Computing Center in Strasbourg.

## RESULTS

### *$^1H$ spectra*

In DMAc/DMF only two partly resolved lines are recorded, which can be attributed to the two environments of a $CH_2$ group with either two $CF_2$ neighbours (main peak) or one $CH_2$ and one $CF_2$ neighbour (minor peak). Their relative intensities are given in *Table 1*. In dioxane the $^1H$ spectrum is resolved at the pentad level, as discussed by Cais[7].

### *$^{19}F$ spectra*

Spectra in DMF/DMAc of two $VF_2$–$VF_4$ copolymers with extreme $VF_4$ contents but still soluble (97/3 and 63/37) are given in *Figure 1*. The three regions around −92, −112 and −126 ppm clearly correspond to $CF_2$ groups with respectively two $CH_2$, one $CH_2$ and one $CF_2$ or two $CF_2$ neighbouring groups. In each of these regions a number of lines are well resolved corresponding to increasingly longer sequences of $CF_2$ and $CH_2$ groups. The possible sequences of three (triads), five (pentads) and seven (heptads) $CH_2$ and $CF_2$ groups that can be found in $VF_2$–$VF_4$ copolymers, taking into account the two types of addition of $VF_2$, have been enumerated by Cais[7]. They are repeated in *Table 2*, where we have adopted the same symbols ($CH_2 = 0$, $CF_2 = 2$) and the same numbering. They take into account the fact that each unsymmetrical carbon sequence is observationally equivalent to its reverse sequence. The positions of the 26 heptads as predicted by Cais[7] are indicated on the enlarged spectra of the 68/32 copolymer in *Figure 2*. It is clear that some are partly resolved. Since, however, some of the minor lines have areas smaller than $10^{-3}$ of the total integrated area, one cannot exclude that some of them may be due to a small amount of chemical defects such as ternary carbons arising from branching, double bonds arising from dehydrofluorination, or end-groups (although the degrees of polymerization are in all cases larger than $10^3$).

Spectra recorded in dioxane show lower resolution in the signals originating from 020 and 222 triads. A typical example is given in *Figure 3*. The resolution in the signals originating from the 022 triads seems improved, in contrast with a complete separation of heptads 10 to 14, which are not well resolved in DMAc/DMF. Noticeable is an inversion in the position of lines 1 and 3 and lines 4 and 5 in the two solvents.

**Table 2** $CF_2$-centred triads, pentads and heptads. Star-labelled sequences should be completed by the observationally equivalent reversed sequence

| Triads | Pentads | Heptads | Number | $\delta$ (ppm from $CFCl_3$) |
|---|---|---|---|---|
| 020 | 20202 | 0202020 | 1 | −91.6 |
| (*a*) | | 0202022* | 2 | −92 |
| | | 2202022 | 3 | −93.6 |
| | 20200* | 2202002* | 4 | −95.9 |
| | (*d*) | 0202002* | 5 | −95.1 |
| 022* | 20222* | 2202220* | 6 | −109.7 |
| (*b*) | | 2202222* | 7 | −110.1 |
| | | 0202222* | 8 | −111.1 |
| | | 0202220* | 9 | −110.7 |
| | 00222* | 2002220* | 10 | −112.6 |
| | (*e*) | 2002222* | 11 | −112.6 |
| | 20220* | 0202202* | 12 | −113.3 |
| | | 0202200* | 13 | −113.0 |
| | | 2202202* | 14 | −113.0 |
| | | 2202200* | 15 | −115.4 |
| | 00220* | 2002202* | 16 | −115.6 |
| | (*f*) | 2002200* | 17 | −115.1 |
| 222 | 22222 | 2222222 | 18 | −121.5 |
| (*c*) | (*g*) | 0222222* | 19 | −120.9 |
| | | 0222220 | 20 | −120.7 |
| | 22220* | 2222202* | 21 | −122.4 |
| | | 0222202* | 23 | −123.1 |
| | | 0222200* | 24 | −122.8 |
| | | 2222200* | 25 | −122.01 |
| | 02220 | 2022202 | 22 | fine structure |
| | | 0022202* | 26 | −124 |
| | | | | −126 |

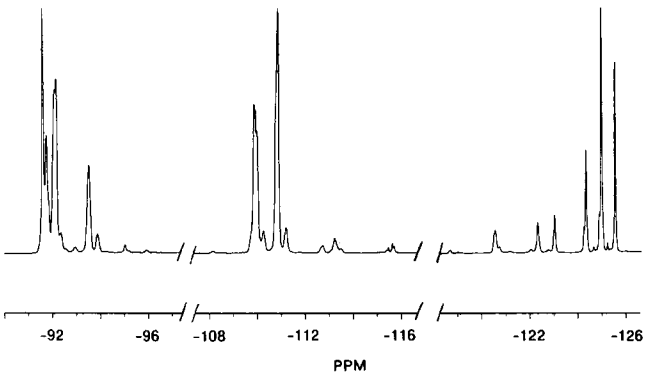


**Figure 2** Enlargements of regions a, b, c of the $^{19}F$ n.m.r. spectrum of the copolymer 70/30

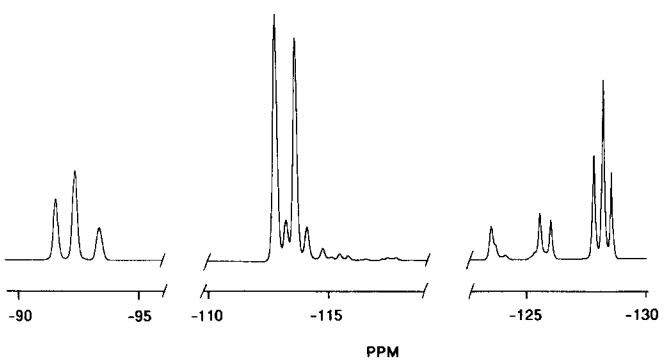


**Figure 3** $^{19}F$ n.m.r. spectrum of copolymer 68/32 in dioxane

## FROM THE SIGNALS TO THE MONOMER SEQUENCES

Cais[7] has shown how to relate the probability of a given odd sequence of carbon nuclei $S_{2n-1}$ to the sequences of monomers $S_{2n}$ from which they can originate, by inspection of the sequences obtained by addition of a $-CH_2-$ or a $-CF_2-$ on either side of the $S_{2n-1}$ sequence. We recall below the relations found for the 0- and 2-centred triads and the 2-centred pentads. The $VF_4$ monomer designated by T contributes a block 22 to the sequence; the $VF_2$ monomer contributes either a block 02 to the sequence for a forward (F) placement or a block 20 for a reverse (R) placement. Therefore:

$$\left.\begin{aligned} p(202)&=\tfrac{1}{2}[p(RR)+p(RT)+p(FF)+p(TF)] \\ p(200)&=\tfrac{1}{2}p(RF) \\ p(002)&=\tfrac{1}{2}p(RF) \end{aligned}\right\}$$

$$\left.\begin{aligned} p(020)&=\tfrac{1}{2}[p(FF)+p(RR)] \qquad a \\ p(022)&=\tfrac{1}{2}[p(FR)+p(FT)+p(RT)] \\ p(220)&=\tfrac{1}{2}[p(FR)+p(TF)+p(TR)] \qquad b \\ p(222)&=\tfrac{1}{2}[p(TR)+p(FT)+2p(TT)] \qquad c \end{aligned}\right\}$$

$$\left.\begin{aligned} p(20200)&=\tfrac{1}{2}p(RRF) \\ p(00202)&=\tfrac{1}{2}p(RFF) \qquad d \\ p(00222)&=\tfrac{1}{2}p(RFT) \\ p(22200)&=\tfrac{1}{2}p(TRF) \qquad e \\ p(00220)&=\tfrac{1}{2}p(RFR) \\ p(02200)&=\tfrac{1}{2}p(FRF) \qquad f \end{aligned}\right\}$$

$$\left.\begin{aligned} p(20220)&=\tfrac{1}{2}[p(RTF)+p(FFR)+p(TFR)] \\ p(02202)&=\tfrac{1}{2}[p(FRR)+p(FRT)+p(RTF)] \qquad h \end{aligned}\right\}$$

$$p(22222)=\tfrac{1}{2}[2p(TTT)+p(TTR)+p(FTT)] \qquad g$$

The problem is now to extract from the $^1H$ signals (as given in *Table 1*) and from the intensities of the easy-to-record $a, b, c, d, e, f, g$ groups of lines (see *Figures 1* and *2*) the following:

(i) the content of the polymer in R, F and T units;

(ii) the probabilities of occurrence $p(ij)$ of the nine possible pairs of monomers.

In fact, the probability of 0-centred triads can be deduced from the probabilities of the 2-centred triads and pentads according to:

$$\begin{aligned} p(0)&=p(00)+p(02) \\ &=p(000)+p(002)+p(020)+p(022) \\ &=0+p(0020)+p(0022)+a+b/2 \\ &=p(00200)+p(00202)+p(00222)+p(00220) \\ &=+a+b/2 \\ &=0+(d+e+f)/2+a+b/2 \end{aligned}$$

Therefore:

$$\begin{aligned} p(002)+p(200)&=d+e+f \\ p(202)&=p(0)-[p(002)+p(200)] \\ &=a+b/2-(d+e+f)/2 \end{aligned}$$

The integrated intensity of all 0- and 2-centred triads can be calculated as:

$$\begin{aligned} N&=(a+b+c)+(a+b/2)-(a+e+f)/2+(d+e+f) \\ &=2a+3b/2+c+(d+e+f)/2 \end{aligned}$$

and

$$\begin{aligned} p(VF_2)&=p(R)+p(F)=2p(0) \\ &=(2a+b+d+e+f)/N \end{aligned}$$

We now have eight independent relations linking the nine $p(ij)$ to the intensities $a, b, c, d, e, f$:

$$\begin{aligned} p(RR)+p(RF)+p(RT)+p(FR)&+p(FF)+p(FT) \\ &=2a+b+(d+e+f)/N \end{aligned}$$

$$\begin{aligned} p(RR)+p(RF)+p(RT)+p(FR)+p(FF)&+p(FT)+p(TR)+p(TF)+p(TT) \\ &=1 \end{aligned}$$

$$p(RF)=(d+e+f)/N$$

$$p(RR)+p(FF)=2a/N$$

$$p(RT)+p(FR)+p(FT)=2b/N$$

$$p(FR)+p(TR)+p(TF)=2b/N$$

$$p(FT)+p(TR)+2p(TT)=2c/N$$

$$p(RT)+p(TF)=b-(d+e+f)/N$$

This is short of one relation to solve the linear system directly. We have either to postulate some value of $p(R)/p(F)$ using values obtained in the $VF_2$ homopolymer or to postulate a kinetic process that allows us to use separately some of the recorded pentad signals and check the consistency at the pentad and heptad level.

The simplest possible polymerization scheme would be

a simple Bernoulli process with $p(ij)=p(i)p(j)$. For such a process we have directly:

$$p(\mathrm{R})+p(\mathrm{F})=2a+b+(d+e+f)/N$$
$$p(\mathrm{R})p(\mathrm{F})=(d+e+f)/N$$
$$p(\mathrm{T})=1-p(\mathrm{R})+p(\mathrm{F})$$

This can be seen to be incompatible with the results.

We can then use a first-order Markov process for which $p(ij)=p(i)P(i|j)$ where $P(i|j)$ is the conditional probability of addition. This process is completely defined by the three $p(i)$ and the nine $P(i|j)$, which introduce three additional relations:

$$P(\mathrm{R}|\mathrm{R})+P(\mathrm{R}|\mathrm{F})+P(\mathrm{R}|\mathrm{T})=1$$
$$P(\mathrm{F}|\mathrm{R})+P(\mathrm{F}|\mathrm{F})+P(\mathrm{F}|\mathrm{T})=1$$
$$P(\mathrm{T}|\mathrm{R})+P(\mathrm{T}|\mathrm{F})+P(\mathrm{T}|\mathrm{T})=1$$

For such a process an additional simple relation relates $p(\mathrm{TT})$ to the pentad signal $g$. Indeed one has:

$$\begin{aligned}2g&=2p(\mathrm{TTT})+p(\mathrm{TTR})+p(\mathrm{FTT})\\&=[2p(\mathrm{TT})P(\mathrm{T}|\mathrm{T})+p(\mathrm{T})P(\mathrm{T}|\mathrm{T})P(\mathrm{T}|\mathrm{R})+p(\mathrm{FT})P(\mathrm{T}|\mathrm{T})]\\&=[2p(\mathrm{TT})P(\mathrm{T}|\mathrm{T})+p(\mathrm{T})P(\mathrm{T}|\mathrm{R})P(\mathrm{T}|\mathrm{T})+p(\mathrm{FT})P(\mathrm{T}|\mathrm{T})]\\&=[2p(\mathrm{TT})+p(\mathrm{TR})+p(\mathrm{FT})]P(\mathrm{T}|\mathrm{T})\\&=2cP(\mathrm{T}|\mathrm{T})\end{aligned}$$

Therefore:

$$P(\mathrm{T}|\mathrm{T})=g/c$$

and

$$\frac{g}{c}p(\mathrm{TR})+\frac{g}{c}p(\mathrm{TF})+\left(\frac{g}{c}-1\right)p(\mathrm{TT})=0$$

The linear system can therefore be resolved. However, the uncertainties in the values of the intensities may lead to negative values for some of the small $p(ij)$, so that adjustments of $p(\mathrm{R})$ may be an easier way. As starting values for $p(\mathrm{R})$ we can choose (i) a fixed proportion of $p(\mathrm{R})$ with respect to $p(\mathrm{R})+p(\mathrm{F})$, or (ii) $p(\mathrm{RR})=0$, i.e. $p(\mathrm{R})=p(\mathrm{RF})+p(\mathrm{RT})=(d+e+f)/N$. The first choice corresponds to the calculation of Cais[7]. We have used the second (reducing to seven the number of independent relations based on $a, b, c, d, e, f$) and solved for the eight remaining $p(ij)$ using the additional relation based on the intensity $g$.

The reliability of the calculation can be appreciated from a comparison of the calculated and observed intensities of the pentads. They are presented as histograms (*Figure 4*) for the main pentads, which have not been directly used in the calculation, i.e. $p(20202)=a-d$, $p(22222)=g$, $p(20222)=b-(e+f+h)$, $p(22220)=k$, $p(02220)=l$. The agreement is fair.

From the values of the pentad intensities, one can

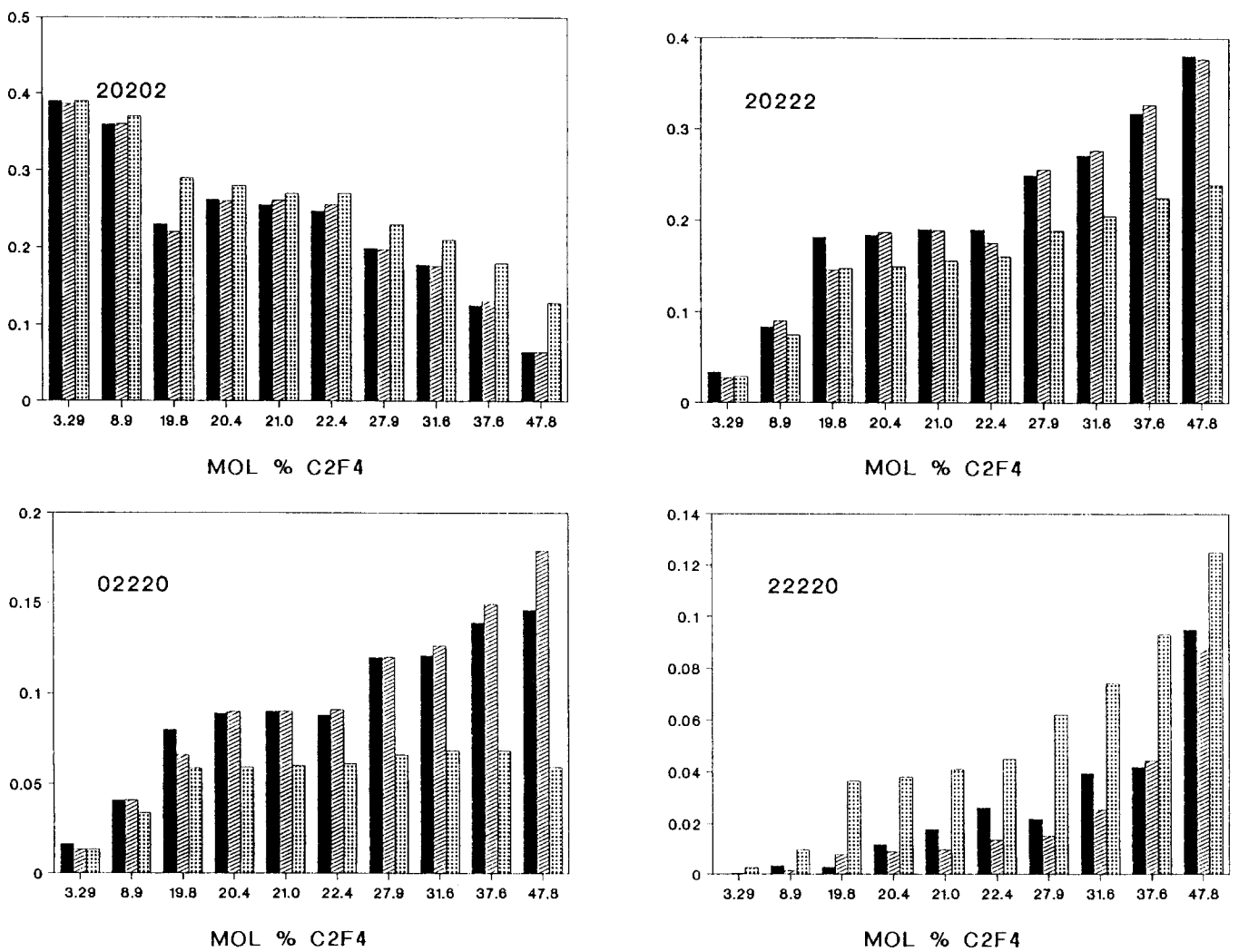


**Figure 4** Comparison of the measured (grey, centre bars) and calculated intensities of the $^{19}F$ n.m.r. signals originating from pentads according to Bernoullian (light grey, right-hand bars) or first-order Markov (black bars) processes

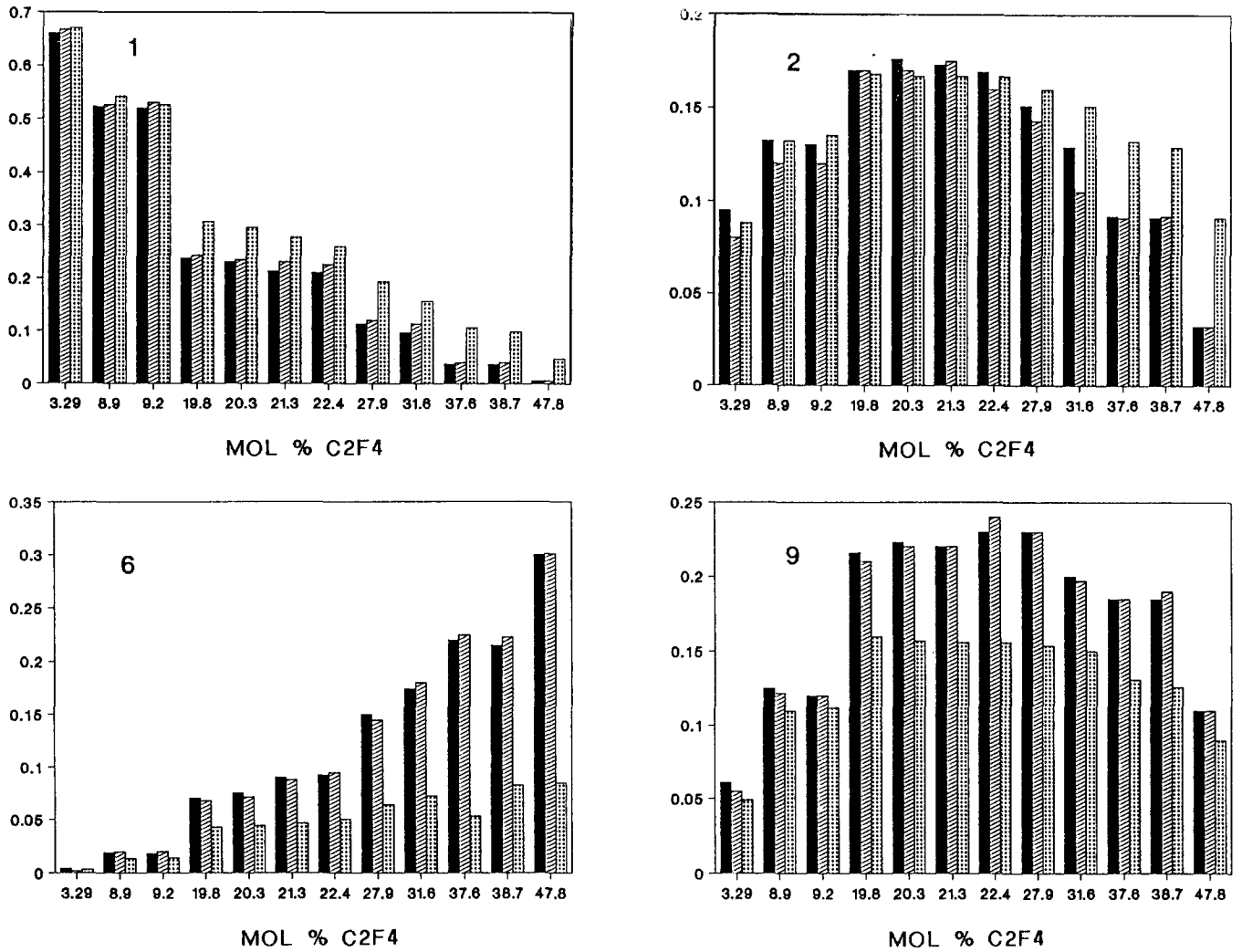


**Figure 5** Comparison of the measured (grey, centre bars) and calculated intensities of the $^{19}F$ n.m.r. signals originating from heptads according to Bernoullian (light grey, right-hand bars) or first-order Markov (black bars) processes

calculate the conditional probabilities $P(i|j)$, recalculate from them the sequences of four monomers and deduce the intensities of the 26 heptads. The probability of occurrence of a given heptad is easily related to the probabilities of occurrence of sequences of four monomers by adding a 0 or 2 before and after the heptad. For example[7]:

$$p(2202202) = p(2022022)$$

$$\begin{aligned} p(2202202) &= [p(22022020) + p(22022022) \\ &\quad + p(02202202) + p(22202202)]/2 \\ &= [p(\text{TFRR}) + p(\text{TFRT}) + p(\text{FRTF}) \\ &\quad + p(\text{TRTF})]/2 \end{aligned}$$

$$\begin{aligned} p(2022022) &= [p(20220220) + p(20220222) \\ &\quad + p(02022022) + p(22022022)]/2 \\ &= [p(\text{RTFR}) + p(\text{RTFT}) + p(\text{FFRT}) \\ &\quad + p(\text{TFRT})]/2 \end{aligned}$$

The intensity of line 14 is therefore

$$\begin{aligned} Int\ 14 = [&p(\text{TFRR}) + 2p(\text{TFRT}) + p(\text{FRTF}) \\ &+ p(\text{TRTF}) + p(\text{RTFR}) + p(\text{RTFT}) \\ &+ p(\text{FFRT})]/2 \end{aligned}$$

These tedious calculations are easily performed by a computer program. The comparison of the calculated and observed intensities is given in *Figure 5* for those lines which are not strongly overlapping in DMAc/DMF. The agreement is very good. This implies that the attributions given by Cais[7] are correct, that a first-order Markov process describes properly the polymerization kinetics and that reliable values of the $P(i|j)$ have been obtained. These are given in *Figure 6*. We can compare them with the values expected from Bernoullian statistics. Values of $P(i|j)$ reported in *Table 3* show reasonable evidence of the preference of F addition to T and of T addition to F, i.e. a tendency towards alternation as compared to blocks of F and T.

This can be put more quantitatively by evaluating the average length of the $VF_2$ and $VF_4$ sequences $\bar{n}_{VF_2}$ and $\bar{n}_{VF_4}$, which can be calculated from:

$$\bar{n}_{VF_2}/2 = \frac{p(\text{RR}) + p(\text{RF}) + p(\text{FR}) + p(\text{FF}) + [p(\text{RT}) + p(\text{FT}) + p(\text{TR}) + p(\text{TF})]/2}{p(\text{RT}) + p(\text{FT}) + p(\text{TR}) + p(\text{TF})}$$

$$\bar{n}_{VF_4}/2 = \frac{p(\text{TT}) + [p(\text{TF}) + p(\text{TR}) + p(\text{RT}) + p(\text{FT})]/2}{p(\text{RT}) + p(\text{FT}) + p(\text{TR}) + p(\text{TF})}$$

where the numerator takes care of all pairs of monomers containing $VF_2$ or $VF_4$ units and the denominator is the

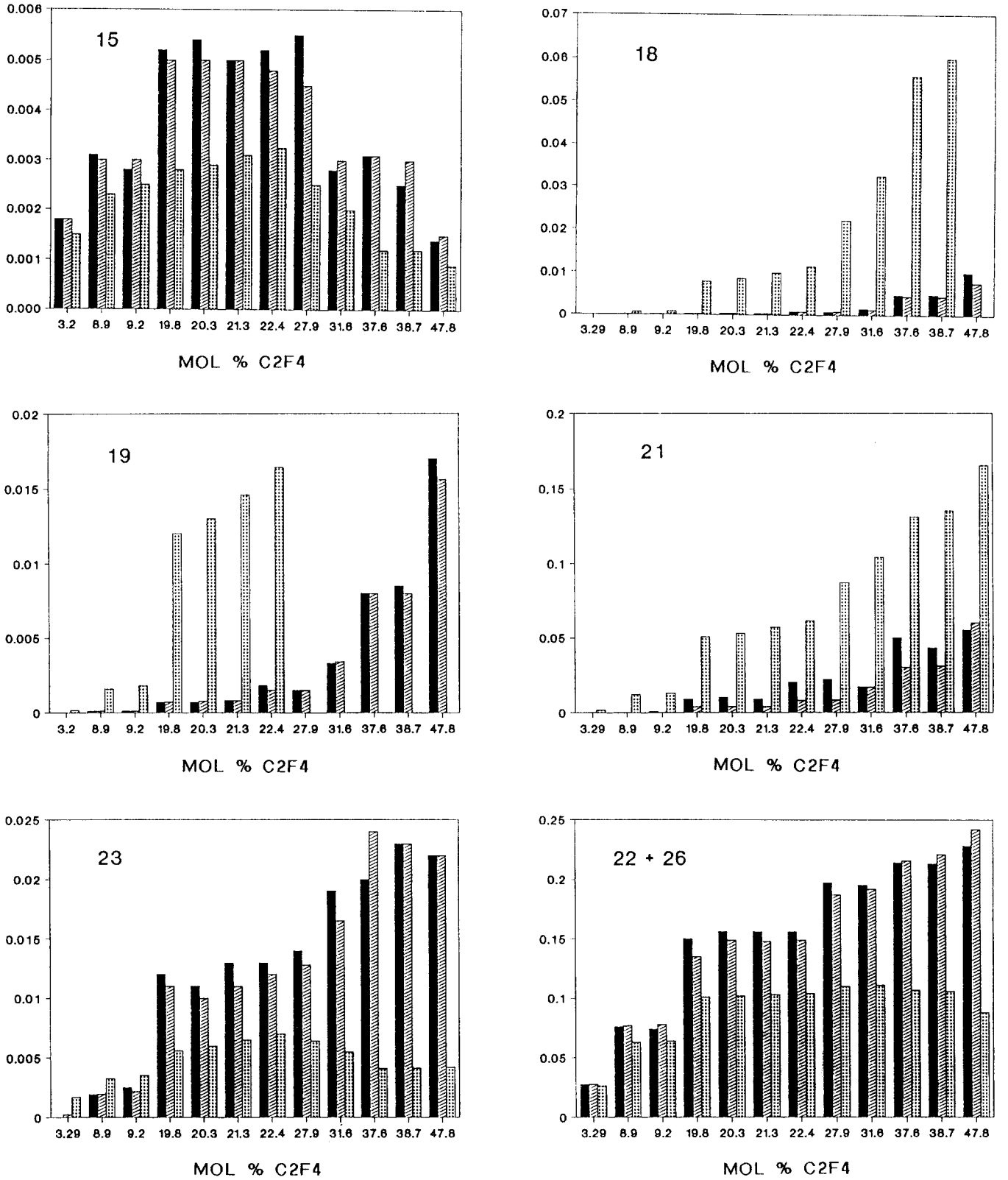


**Figure 5** *Continued*

number $N_{VF_2VF_4}$ of pairs separating a $VF_2$ and a $VF_4$ sequence. The results are given in *Figure 7*. *Figure 8* represents the factor $\chi$ defined by Koenig[9] as a way to measure the departure from random statistics:

$$\chi \bar{n}_{VF_2} \bar{n}_{VF_4} N_{VF_2VF_4} = 2$$

It may also be interesting to characterize the role of certain sequences in inducing the changes of structure observed by Lovinger *et al.*[4]. Of major interest are the sequences derived from the 222 triads, which give signals in the $-120$ to 127 ppm region. Examination of *Figure 9* reveals that this region is much more resolved than the pentad level and it has been found worth while to try to attribute the lines beyond the heptad level:

(i) to check the consistency of our calculation; and

(ii) to use them as additional data for the refinement of the $P(i|j)$ values.

In fact the lines corresponding to the 02222 and 22222 pentads have very low intensities in the soluble $VF_2$–$VF_4$ polymers (a consequence of the tendency of the $VF_4$ units

to be isolated) and are hardly resolved at the heptad levels (lines 18, 19, 20, 21, 23, 24, 25).

Some lines derived from the 02220 pentad are, on the contrary, intense and very well resolved. Heptad 26 always has a very low probability since it implies the presence of an R monomer:

$$p(0022202)+p(2022200)$$
$$=p(20022202)/2+p(20222002)/2$$
$$=p(\mathrm{RFTF})+p(\mathrm{RTRF})$$

On the contrary, heptad 22 arises from some R-free

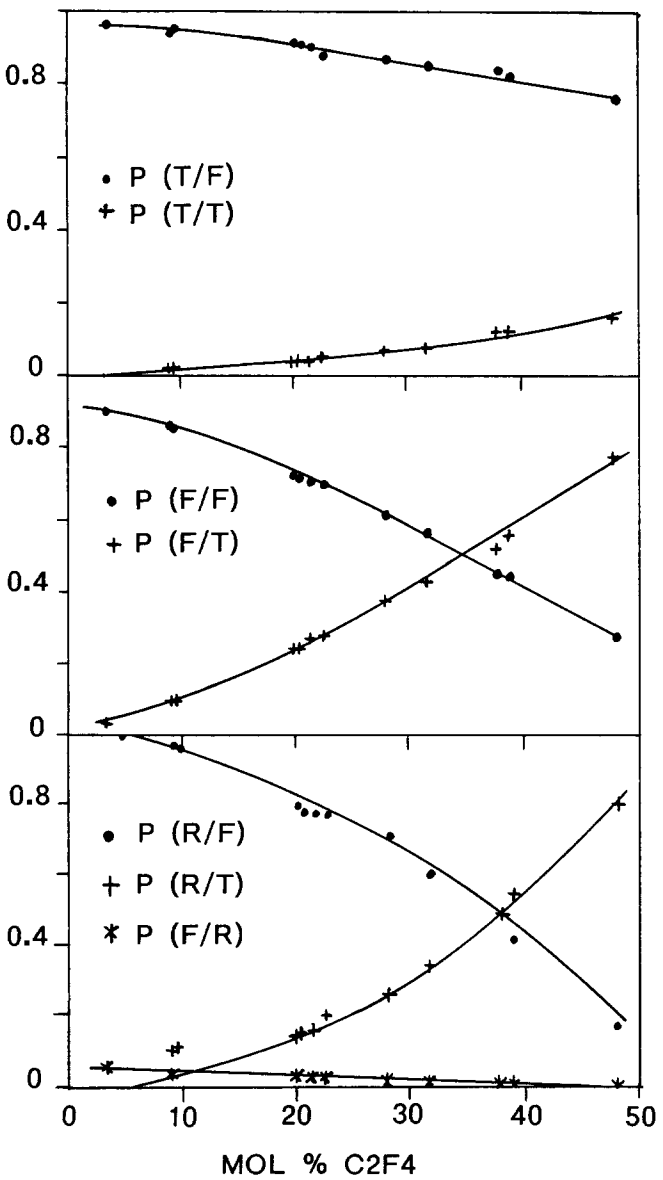


**Figure 6** Variation of the conditional probabilities of addition $P(i|j)$ as a function of $VF_4$ content

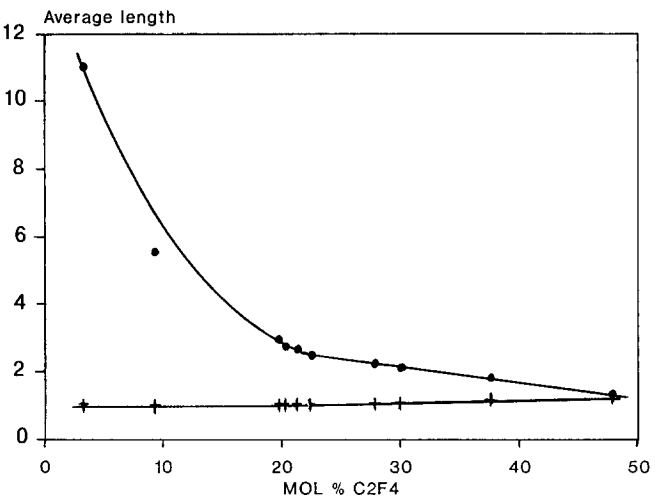


**Figure 7** Mean length $\bar{n}$ of the $VF_2$ (●) and $VF_4$ (+) sequences as a function of $VF_4$ content

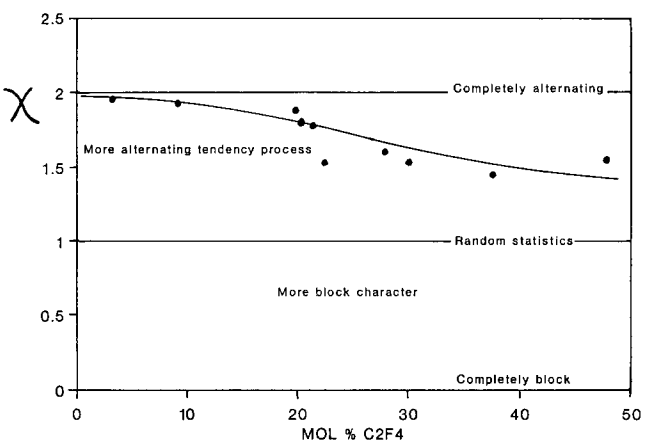


**Figure 8** Departure of the sequence distribution from Bernoullian statistics as a function of $VF_4$ content

**Table 3** Mean values of the conditional probabilities $P(i|j)$

| $VF_4$ (%) | F\|F | F\|R | F\|T | R\|F | R\|R | R\|T | T\|F | T\|R | T\|T |
|---|---|---|---|---|---|---|---|---|---|
| 3.3 | $0.90_2$ | 0.057 | 0.039 | 0.97 | 0.053 | ≃0 | 0.96 | 0.039 | ≃0 |
| 9.2 | 0.85 | 0.040 | 0.10 | 0.97 | 0.038 | ≃0 | 0.95 | 0.035 | 0.02 |
| 19.8 | 0.71 | 0.049 | 0.24 | 0.80 | 0.032 | 0.16 | 0.95 | 0.045 | 0.03 |
| 21.4 | 0.72 | 0.039 | 0.24 | 0.80 | 0.034 | 0.16 | 0.94 | 0.049 | 0.04 |
| 21.3 | 0.70 | 0.032 | 0.26 | 0.80 | 0.036 | 0.16 | 0.92 | 0.050 | 0.03 |
| 22.4 | 0.69 | 0.031 | 0.28 | 0.78 | 0.034 | 0.17 | 0.89 | 0.057 | 0.06 |
| 28.0 | 0.61 | 0.032 | 0.36 | 0.71 | 0.028 | 0.027 | 0.88 | 0.062 | 0.07 |
| 31.6 | 0.56 | 0.028 | 0.43 | 0.61 | 0.027 | 0.37 | 0.86 | 0.060 | 0.08 |
| 37.7 | 0.44 | 0.019 | 0.52 | 0.48 | 0.014 | 0.51 | 0.88 | 0.060 | 0.12 |
| 47.8 | 0.26 | ≃0 | 0.76 | 0.18 | 0.010 | 0.82 | 0.76 | 0.078 | 0.10 |

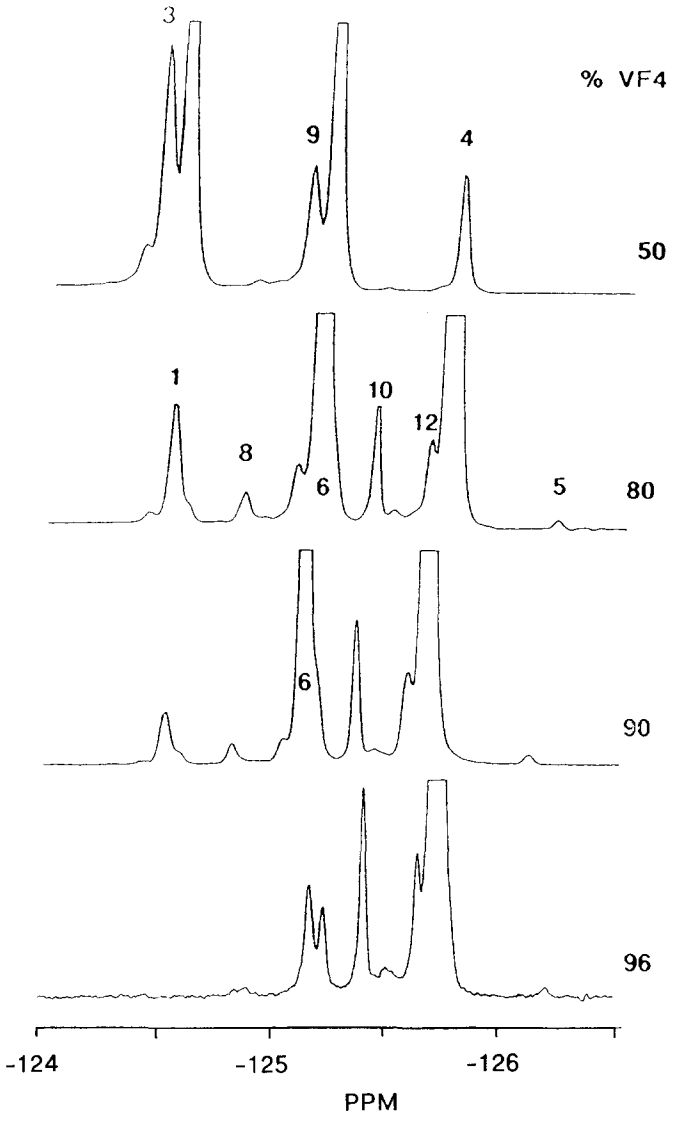


**Figure 9** $^{19}F$ n.m.r. spectrum of the region $-124$ to $-127$ ppm showing the resolution at the undecad level of the signals originating from the 02220 pentad and their variations with increasing $VF_4$ content (see *Tables 4* and *5*)

sequences since:

$$p(2022202) = p(22022202) + p(02022202) + p(20222020) + p(20222022) = p(TFTF) + p(FFTF) + p(RTRR) + p(RTRT)$$

The first two terms have rather large probabilities, which explains the number of lines that can be observed at the nonad and undecad level (*Table 4*).

The evolution of the spectra (*Figure 9*) with increasing $VF_4$ content can be compared with the calculated values according to the first-order Markov process (*Table 5*) to attribute the nine observable lines. The agreement is not fully quantitative and one could use these intensities to refine the values of $p(i)$ and of the $P(i|j)$. This is left to further work but it may be very interesting to use signals in a narrow range of chemical shift with strong variations in intensity as a fingerprint for the characterization of the microstructure of $VF_2$–$VF_4$ copolymers of similar composition but different copolymerization process.

**Table 4** Heptads, nonads and undecads from the 02220 pentad. Signals from nonads in italics are shown in *Figure 9*

| Heptad | Nonad | Undecad | |
|---|---|---|---|
| 2022202 | 220222022 | 22202220222 | *U1* |
| | N1 | 02202220220 | *U2* |
| | | 22202220220* | *U3* |
| | 020222020 | 20202220202 | *U4* |
| | N2 | 00202220202* | *U5* |
| | 220222020* | 22202220202* | *U6* |
| | N3 | 02202220200* | *U7* |
| | | 22202220200* | *U8* |
| | | 02202220202* | *U9* |
| 0022202 | 200222020* | 22002220202* | *U10* |
| | N4 | 02002220202* | *U11* |
| | 200222022* | 22002220222* | *U12* |
| | N5 | 02002220220* | *U13* |
| | | 22002220220* | *U14* |
| | | 02002220222* | *U15* |

**Table 5** Calculated probabilities[a] of undecads U1 to U15

| $VF_4$ (%) | 3.3 | 9.2 | 19.8 | 21.4 | 28 | | | |
|---|---|---|---|---|---|---|---|---|
| U1 | 0.001 | 0.01 | 0.058 | 0.067 | $0.13_7$ | $0.18_1$ | 0.30 | 0.56 |
| U2 | 0.002 | $\simeq 0$ | $\simeq 0$ | $\simeq 0$ | $\simeq 0$ | $\simeq 0$ | $\simeq 0$ | $\simeq 0$ |
| U3 | 0.002 | 0.004 | 0.009 | 0.012 | 0.015 | 0.007 | 0.01 | $\simeq 0$ |
| U4 | 0.77 | 0.70 | 0.49 | 0.46 | 0.34 | 0.30 | 0.19 | 0.065 |
| U5 | 0.05 | 0.03 | 0.019 | 0.017 | 0.01 | 0.008 | $0.003_5$ | $\simeq 0$ |
| U6 | 0.05 | 0.16 | 0.34 | 0.36 | 0.43 | $0.46_5$ | 0.47 | 0.38 |
| U7 | 0.002 | $0.001_3$ | $0.001_4$ | 0.001 | $\simeq 0$ | $\simeq 0$ | $\simeq 0$ | $\simeq 0$ |
| U8 | 0.001 | $0.003_5$ | $0.005_7$ | 0.008 | 0.007 | 0.006 | 0.004 | $0.001_5$ |
| U9 | 0.05 | $0.003_5$ | $0.003_8$ | $0.002_5$ | $0.02_5$ | 0.009 | 0.01 | $\simeq 0$ |
| U10 | 0.05 | 0.004 | 0.003 | 0.003 | 0.020 | 0.015 | 0.009 | 0.002 |
| U11 | $\simeq 0$ | $\simeq 0$ | $\simeq 0$ | $\simeq 0$ | $\simeq 0$ | $\simeq 0$ | $\simeq 0$ | $\simeq 0$ |
| U12 | 0.002 | $0.004_5$ | 0.01 | 0.01 | 0.013 | 0.012 | 0.011 | 0.007 |
| U13 | 0.002 | $\simeq 0$ | $\simeq 0$ | $\simeq 0$ | $\simeq 0$ | $\simeq 0$ | $\simeq 0$ | $\simeq 0$ |
| U14 | 0.004 | 0.002 | $0.001_6$ | $0.001_6$ | 0.001 | $\simeq 0$ | $\simeq 0$ | $\simeq 0$ |
| U15 | 0.001 | $\simeq 0$ | $\simeq 0$ | $\simeq 0$ | $\simeq 0$ | $\simeq 0$ | $\simeq 0$ | $\simeq 0$ |

[a] Probabilities $< 10^3$ have been reported $\simeq 0$

A few other heptads in other regions show significant resolution and can be eventually resolved:

(i) heptad 3 gives two nonads, 022020222 at −93.5 and 222020222 at −93.8 ppm;

(ii) heptad 6 gives four nonads, 222022200 at −109.6 ppm, 222022202 at −109.7 ppm, 0222022200 at 109.8 ppm and 022022202 at −109.9 ppm; and

(iii) heptad 9 gives two nonads, 202022202 at −110.8 ppm and 002022202 at −110.9 ppm.

## CONCLUSIONS

Our analysis of the high-resolution $^{19}F$ n.m.r. of $VF_2$–$VF_4$ copolymers in a large range of composition confirms that the copolymerization kinetics obeys a first-order Markov process and extends beyond this. The calculation of the conditional probabilities of addition demonstrates the tendency of $VF_4$ units to remain isolated. The sequences centred on $VF_4$ units can be analysed up to a succession of 11 carbons. Such detailed knowledge may be useful to understand the changes in crystalline structure, melting temperature and Curie point with increasing $VF_4$ content.

## ACKNOWLEDGEMENTS

This work has been supported by Atochem through a grant to one of us (G.L.) and the gift of the samples synthesized by M. Kappler, which have been used throughout this work. The help of Dr R. Graff in recording the $^{19}F$ spectra is gratefully acknowledged. Thanks are due to Professor A. Bieber for his help in setting up a program for computation of the Markov parameters.

## REFERENCES

1 Farmer, B. L., Hopfinger, A. J. and Lando, J. B. *J. Appl. Phys.* 1972, **43**, 4293
2 Lovinger, A. J., Davis, D. P., Cais, R. E. and Kometani, J. M. *Polymer* 1987, **28**, 617
3 Lando, J. B. and Doll, W. W. *J. Macromol. Sci.–Phys. (B)* 1968, **2**, 205
4 Lovinger, A. J., Davis, D. P., Cais, R. E. and Kometani, J. M. *Macromolecules* 1988, **21**, 78
5 Wilson, C. W. and Santee, E. R. *J. Polym. Sci. (C)* 1965, **8**, 97
6 Murasheva, Y. M., Shashkov, A. I. and Dontsov, A. A. *Polym. Sci. USSR* 1981, **23**, 711
7 Cais, R. E. and Kometani, J. M. *Anal. Chim. Acta* 1986, **189**, 101
8 Lutringer, G. and Weill, G. *Polymer* 1991, **32**, 877
9 Koenig, J. L. in 'Chemical Microstructure of Polymer Chains', Wiley, New York, 1980